

# A Shortcut to Finite-time Memory Erasure

Geng Li<sup>1,2</sup> and Hui Dong<sup>1,\*</sup>

<sup>1</sup>Graduate School of China Academy of Engineering Physics, Beijing 100193, China

<sup>2</sup>School of Systems Science, Beijing Normal University, Beijing 100875, China

To achieve fast computation, it is crucial to reset the memory to a desired state within a limited time. However, the inherent delay in the system's response often prevents reaching the desired state once the control process is completed in finite time. To address this challenge, we propose a shortcut strategy that incorporates an auxiliary control to guide the system towards an equilibrium state that corresponds to the intended control, thus enabling accurate memory reset. Through the application of thermodynamic geometry, we derive an optimal shortcut protocol for erasure processes that minimizes the energy cost. This research provides an effective design principle for realizing the finite-time erasure process while simultaneously reducing the energy cost, thereby alleviating the burden of heat dissipation.

**Introduction.** – Memory erasure is an essential step in computations with an unavoidable energy cost. Landauer's principle posts a fundamental lower bound on the energy cost of erasing a one-bit memory carried out infinitely slowly [1–3]. However accelerating computing processes typically requires to complete memory erasure in finite time. There is an inevitable trade-off between erasure speed and accuracy when rapidly initializing the memory system. In such a finite-time thermodynamic process, a system often does not immediately respond to external perturbation, resulting in a lag between the final state and the desired equilibrium state [4, 5]. This systematic state lag poses a significant challenge in initializing the system to the target state promptly [6–12], and also leads to a substantial increase in energy costs when the erasure time is reduced [13–24]. The quest to achieve rapid erasure with minimal energy costs drives us to design alternative memory erasure strategies.

Much effort has been devoted to reduce the state lag developed in nonequilibrium driving processes [25–31]. As a promising candidate, shortcut to isothermality was proposed as a finite-time driving strategy to escort the system evolving along a series of instantaneous equilibrium states [31] with the application to realize fast transitions between equilibrium states [32, 33], improve free energy calculations [34, 35], and design Brownian heat engines [36–39]. As shown in Fig. 1, we adopt such shortcut strategy to design a finite-time erasure protocol to reset a classical memory. And the thermodynamic geometric approach [40–42] is used to design the optimal protocol with the minimal energy cost.

**Shortcuts to memory erasure.** – The memory as a simple binary system can be simplified as a particle in a bistable potential well. Here, we consider a one-bit memory system modeled by a Brownian particle in a double-well potential  $U_o(x, \vec{\lambda}) = kx^4 - A\lambda_1 x^2 - B\lambda_2 x$ , where  $x$  represents the coordinate. And  $k$ ,  $A$ , and  $B$  are constant coefficients introduced to define the dimensionless variables  $\vec{\lambda}(t) \equiv (\lambda_1, \lambda_2)$  as time-dependent control pa-

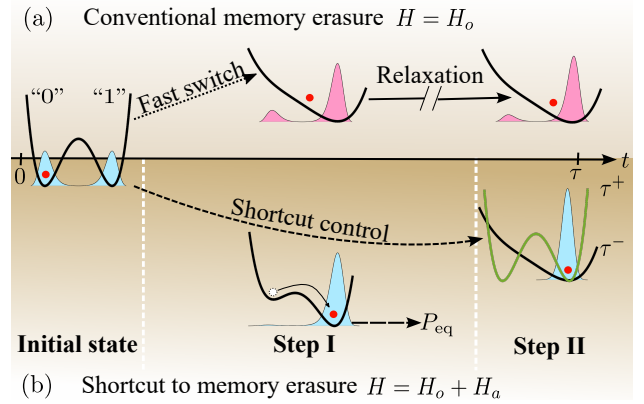


FIG. 1. Schematic of finite-time memory erasure. The one-bit memory is modeled by a physical double-well system. In the initial state, the system stores the state's information “0” or “1”. The task of memory erasure is to reset the system into the blank state “1”. (a) Conventional memory erasure scheme with the Hamiltonian  $H_o$ . The double-well potential is fast switched to fulfill classical memory reset in finite time  $\tau$ . A systematic state lag is accumulated between the system's current state and its corresponding equilibrium state. Therefore, a slow relaxation process is needed to reach the desired erasure accuracy. (b) Shortcut to memory erasure with the Hamiltonian  $H = H_o + H_a$ . In the step I, an auxiliary Hamiltonian  $H_a$  is added to escort the system evolving along the instantaneous equilibrium path of the original Hamiltonian  $H_o$  within finite time. The system is finally expelled into the blank state “1” without accumulation of the state lag. In the step II, the potential is quenched to the double-well form for later computations.

rameters. The evolution of the system is described by Hamiltonian  $H_o(x, p, \vec{\lambda}) \equiv p^2/(2m) + U_o(x, \vec{\lambda})$  with  $p$  as the momentum and  $m$  as the mass of the particle. The memory is encoded by mapping the microstate  $x$  into two macrostates. If the particle is in the left well ( $x < 0$ ), the system is in macrostate “0”. Conversely, if the particle is in the right well ( $x > 0$ ), the system is in macrostate “1”, which serves as the blank state for storing memory.

The system is in contact with a thermal reservoir with a constant temperature  $T$ . The barrier separating the

\* hdong@gscaep.ac.cn

double well is assumed to be much larger than the thermal fluctuation so that the memory can be considered stable [6, 8].

The particle is initially in an equilibrium microstate with the control parameters  $\vec{\lambda}(0) = (1, 0)$  and has the same probability  $1/2$  to stay in each macrostate (0 or 1). The entropy is  $S = k_B \ln 2$  for the initial microstate of the particle with  $k_B$  being the Boltzmann constant. During the Landauer's quasi-static erasure process [1–3], the particle is expelled into macrostate “1” by changing control parameters  $\vec{\lambda}$  slowly to maintain the equilibrium state  $P_{\text{eq}} = \exp[\beta(F - H_o)]$ , where  $F \equiv -\beta^{-1} \ln[\int \int dx dp \exp(-\beta H_o)]$  is the free energy with the inverse temperature  $\beta \equiv 1/(k_B T)$ . And the entropy for the final state is  $S = 0$ . Such reduction of the entropy makes the memory erasure a logically irreversible process. Once the control parameters  $\vec{\lambda}$  are tuned with finite rate as illustrated in Fig. 1 (a), the system is driven to a nonequilibrium state typically with a lag, resulting in a residual entropy  $S > 0$ . And additional relaxation is required to achieve the desired accuracy with the sacrifice of longer time [3, 43, 44].

To meet the need of fast erasure and reduce the lag, we adopt the shortcut scheme where an auxiliary Hamiltonian  $H_a(x, p, t)$  is supplemented to escort the system evolving along the instantaneous equilibrium state  $P_{\text{eq}}$  during the finite-time erasure process with boundary conditions  $H_a(0) = H_a(\tau) = 0$ . The probability distribution  $P(x, p, t)$  of the microstate follows the Kramers equation,

$$\frac{\partial P}{\partial t} = -\frac{\partial}{\partial x} \left( \frac{\partial H}{\partial p} P \right) + \frac{\partial}{\partial p} \left( \frac{\partial H}{\partial x} P + \gamma \frac{\partial H}{\partial p} P \right) + \frac{\gamma}{\beta} \frac{\partial^2 P}{\partial p^2}, \quad (1)$$

where  $H \equiv H_o + H_a$  is the total Hamiltonian and  $\gamma$  is the dissipation coefficient. Our operation of memory erasure, illustrated in Fig. 1 (b), consists two steps as follows.

**Step I, Shortcut Erasure.** The particle is expelled to the right well ( $x > 0$ ) in the finite-time interval  $t \in [0, \tau]$ , by raising the left well, illustrated as the step I in Fig. 1 (b). The control parameters are tuned from  $\vec{\lambda}(0)$  to  $\vec{\lambda}(\tau) = (0, 1)$ . With the strategy of shortcuts to isothermality [31], the system evolves along the path of instantaneous equilibrium states, and reaches the final equilibrium state  $P = P_{\text{eq}}(\tau)$  with the control parameters  $\vec{\lambda}(\tau)$ . The requirement for the auxiliary Hamiltonian  $H_a$  follows as

$$\frac{\gamma}{\beta} \frac{\partial^2 H_a}{\partial p^2} - \frac{\gamma p}{m} \frac{\partial H_a}{\partial p} + \frac{\partial H_a}{\partial p} \frac{\partial H_o}{\partial x} - \frac{p}{m} \frac{\partial H_a}{\partial x} = \frac{dF}{dt} - \frac{\partial H_o}{\partial t}. \quad (2)$$

The auxiliary Hamiltonian is proved to have the form  $H_a(x, p, t) = \dot{\vec{\lambda}} \cdot \vec{f}(x, p, \vec{\lambda})$  with the boundary condition  $\dot{\vec{\lambda}}(0) = \dot{\vec{\lambda}}(\tau) = 0$ .

**Step II, Potential Quench.** For later computation purpose, the potential is reset to the double-well

form. Such operation is realized by quenching the control parameters from  $\vec{\lambda}(\tau^-) = (0, 1)$  to the initial value  $\vec{\lambda}(\tau^+) = (1, 0)$  at the time  $t = \tau$  with an instantaneous change of the system Hamiltonian  $H_o(\tau^-) \rightarrow H_o(\tau^+)$ . Here,  $\tau^-$  and  $\tau^+$  denote the time before and after the potential quench respectively.

After these two steps, the memory is erased to the blank state and the system is reset within finite time  $\tau$  to allow the later usage.

*Geometric erasure protocol.* – Energy cost is inevitable in a finite-time erasure process. We employ the geometric approach [40, 41] to derive the optimal erasure protocol with minimal energy costs. In the shortcut scheme with the total Hamiltonian  $H = H_o + H_a$ , the work performed in the erasure process with duration  $\tau$  is  $W \equiv \langle \int_0^\tau \partial H / \partial t dt \rangle_{\text{eq}}$ , which is explicitly obtained as

$$W_s = \Delta F + \gamma \int_0^\tau dt \langle (\frac{\partial H_a}{\partial p})^2 \rangle_{\text{eq}}, \quad (3)$$

where  $\langle \cdot \rangle_{\text{eq}} \equiv \int \int dx dp [\cdot] P_{\text{eq}}$ . Since the potential quench in the Step II is realized instantaneously, the system distribution remains unchanged. And the work done in this process follows as  $W_q = \int \int dx dp (H_o(\tau^+) - H_o(\tau^-)) P_{\text{eq}}(\tau)$ .

With the explicit form of the auxiliary Hamiltonian  $H_a = \dot{\vec{\lambda}} \cdot \vec{f}$ , the irreversible energy cost of the erasure process is written as

$$\begin{aligned} W_{\text{irr}} &\equiv W - \Delta F - W_q \\ &= \gamma \sum_{\mu\nu} \int_0^\tau dt \dot{\lambda}_\mu \dot{\lambda}_\nu \langle \frac{\partial f_\mu}{\partial p} \frac{\partial f_\nu}{\partial p} \rangle_{\text{eq}}, \end{aligned} \quad (4)$$

with the total work  $W = W_s + W_q$ . Here  $W_q$  is excluded from the irreversible energy cost  $W_{\text{irr}}$  in Eq. (4) since the potential quench in the Step II is a reversible process. In the space of the control parameters  $\vec{\lambda}$ , a semi-positive metric can be defined as  $g_{\mu\nu} \equiv \gamma \langle \partial f_\mu / \partial p \partial f_\nu / \partial p \rangle_{\text{eq}}$  on a Riemannian manifold. The shortest curve connecting two given endpoints in this parametric space is the geodesic line with the distance described by the thermodynamic length [45–48]  $\mathcal{L} \equiv \int_0^\tau dt \sqrt{\sum_{\mu\nu} \dot{\lambda}_\mu \dot{\lambda}_\nu g_{\mu\nu}}$ , which provides a lower bound for the irreversible energy cost  $W_{\text{irr}} \geq \mathcal{L}^2 / \tau$ . Therefore, the geodesic line serves as the optimal erasure protocol with minimal energy costs.

In the shortcut scheme, the auxiliary Hamiltonian  $H_a$  can be solved from Eq. (2) with the given original Hamiltonian  $H_o$ . However, the form of the auxiliary Hamiltonian  $H_a$  generally depends on the particle's momentum [31, 35, 41]. The demand of constantly monitoring the particle's velocity makes it difficult for implementation of momentum-dependent terms in experiment [49, 50]. Here we design a variational auxiliary control  $H_a^* = \dot{\vec{\lambda}} \cdot \vec{f}^*(x, p, \vec{\lambda})$  that is used to replace the exact auxiliary Hamiltonian  $H_a$ , where  $\vec{f}^*$  represents an approxi-

mation to the function  $\vec{f}$  to ensure the minimization of a variational functional as

$$\mathcal{G}(H_a^*) = \int dx dp \left( \frac{\gamma}{\beta} \frac{\partial^2 H_a^*}{\partial p^2} - \frac{\gamma p}{m} \frac{\partial H_a^*}{\partial p} + \frac{\partial H_o}{\partial x} \frac{\partial H_a^*}{\partial p} - \frac{p}{m} \frac{\partial H_a^*}{\partial x} + \frac{\partial H_o}{\partial t} - \frac{dF}{dt} \right)^2 e^{-\beta H_o}. \quad (5)$$

Such variational functional is defined to ensure the minimum discrepancy between evolutions governed by the approximate Hamiltonian  $H_a^*$  and the exact Hamiltonian  $H_a$ . And the variational auxiliary Hamiltonian for the Brownian particle takes the form  $H_a^* = \sum_{\mu=1}^2 \dot{\lambda}_\mu f_\mu^*(x, p, \vec{\lambda})$  with  $f_1^* = a_4 x p + a_3 p + a_2 x^2 + a_1 x$ , and  $f_2^* = b_4 x p + b_3 p + b_2 x^2 + b_1 x$ . Here  $a_n \equiv a_n(\vec{\lambda})$  and  $b_n \equiv b_n(\vec{\lambda})$  with  $n = 1, 2, 3, 4$  are functions to be determined through the variational procedure. With the adoption of the shortcut scheme under the total Hamiltonian  $H = H_o + H_a^*$ , the system can be escorted along a series of near-equilibrium state  $P_{\text{eq}}^* \approx P_{\text{eq}}$ .

With the operation of a gauge transformation  $X = x$  and  $P = p + m \partial H_a^* / \partial p$ , we obtain an equivalent process

$$\dot{X} = \frac{P}{m}, \quad \dot{P} = -\frac{\partial U_o}{\partial X} - \frac{\partial U_a}{\partial X} - \gamma \dot{X} + \xi(t), \quad (6)$$

where  $\xi(t)$  is the Gaussian white noise and the auxiliary potential  $U_a(X, t) = C_2(t)X^2 + C_1(t)X$  is momentum-independent. Detailed derivations of the equivalent process in Eq. (6) and the lengthy expressions of  $C_1(t)$  and  $C_2(t)$  are presented in Supplemental Material [51]. In this equivalent process, the system's distribution follows a fixed pattern

$$P_f(X, P, t) = \exp \left\{ \beta \left[ F - \frac{1}{2m} (P - m \partial H_a^* / \partial p)^2 - U_o \right] \right\}. \quad (7)$$

With the boundary conditions  $\dot{\vec{\lambda}}(0) = \dot{\vec{\lambda}}(\tau) = 0$ , the extra term  $m \partial H_a^* / \partial p$  in Eq. (7) vanishes and the system's distribution  $P_f$  returns to the instantaneous equilibrium distribution  $P_{\text{eq}}^*$  at the beginning  $t = 0$  and end  $t = \tau$  of the driving process.

**Reset errors.** – The conventional approach of memory erasure is to tune the system Hamiltonian  $H_o$  via control parameters  $\vec{\lambda}$ . The memory state evolves accordingly yet with a lag, which induces reset errors especially for the case with short erasure time  $\tau$ . The shortcut scheme with the Hamiltonian  $H = H_o + U_a$  effectively fulfills the demands for both erasure speed and accuracy, without introducing any additional freedom of control.

We numerically obtain the shortcut scheme with the Hamiltonian  $H = H_o + U_a$  and compare it with the conventional scheme with the Hamiltonian  $H' = H_o$  in a one-bit memory erasure process. In simulations, we choose the parameters as  $k = 4$ ,  $A = 8$ ,  $B = 16$ ,  $k_B T = 1$ ,  $\gamma = 1$ , and  $m = 0.01$ . See Supplemental Material for more details about the simulation [51]. A straightforward

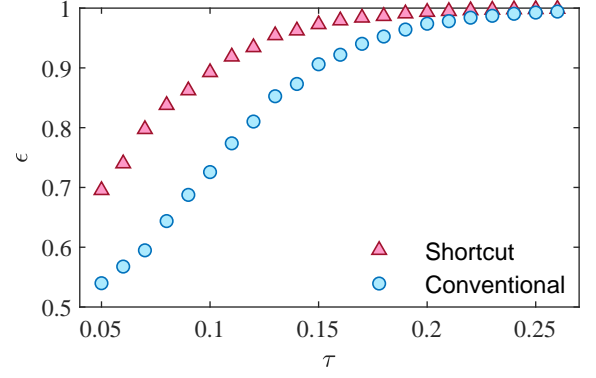


FIG. 2. The erasure accuracy  $\epsilon$  of the shortcut scheme (red triangles) and the conventional erasure scheme (blue circles). The erasure accuracy is defined as the probability of particles ending in the right well  $\epsilon \equiv \int_0^\infty P(x, \tau) dx$ . During the erasure process, the shortcut scheme adopts the Hamiltonian  $H = H_o + U_a$  while the conventional scheme takes the Hamiltonian  $H' = H_o$ . In the simulation, we choose the parameters as  $k = 4$ ,  $A = 8$ ,  $B = 16$ ,  $k_B T = 1$ ,  $\gamma = 1$ , and  $m = 0.01$  and the straightforward control protocol as  $\lambda_1^s(t) = 0.5 + 0.5 \cos(\pi t / \tau)$  and  $\lambda_2^s(t) = 0.5 - 0.5 \cos(\pi t / \tau)$ . The shortcut scheme always ensures high erasure accuracy while the conventional erasure scheme only achieves considerable erasure accuracy at long erasure duration.

control protocol is selected as  $\lambda_1^s(t) = 0.5 + 0.5 \cos(\pi t / \tau)$  and  $\lambda_2^s(t) = 0.5 - 0.5 \cos(\pi t / \tau)$  to continuously meet the boundary conditions. The erasure accuracy is defined as the relative number of particles reaching the right well at the end of the erasure process  $\epsilon \equiv \int_0^\infty P(x, \tau) dx$ . Figure 2 shows the erasure accuracy  $\epsilon$  for different erasure durations  $\tau$ . The accuracy of the shortcut scheme is superior to that of the conventional scheme over different durations. Especially in short erasure time, the conventional scheme almost fails while the accuracy of the shortcut scheme still maintains high level.

**Energy cost optimization.** – In the shortcut scheme, the auxiliary Hamiltonian  $H_a^*$  is obtained once the control protocol  $\vec{\lambda}(t)$  with  $t \in [0, \tau]$  is specified for the conventional erasure process. Among these protocols, one with the minimum energy cost can be found with our geometric methods. We test the geometric approach for minimizing the energy cost of the erasure process. The geodesic protocol is obtained by numerically solving the geodesic equation in the parametric space  $\vec{\lambda}$  with the metric  $g_{\mu\nu}$ . The details on the form of the metric and the geodesic equation are presented in the Supplemental Materials [51]. Figure 3 (a) shows the difference between the geodesic protocol and the above straightforward protocol  $\vec{\lambda}^s(t)$ . In Fig. 3 (b), we compare the irreversible energy cost of the geodesic protocol (green squares) with that of the straightforward protocol (red triangles). The irreversible energy cost  $W_{\text{irr}}$  given by the geodesic protocol is lower than that from the straightforward protocol. Such observation proves the geometric

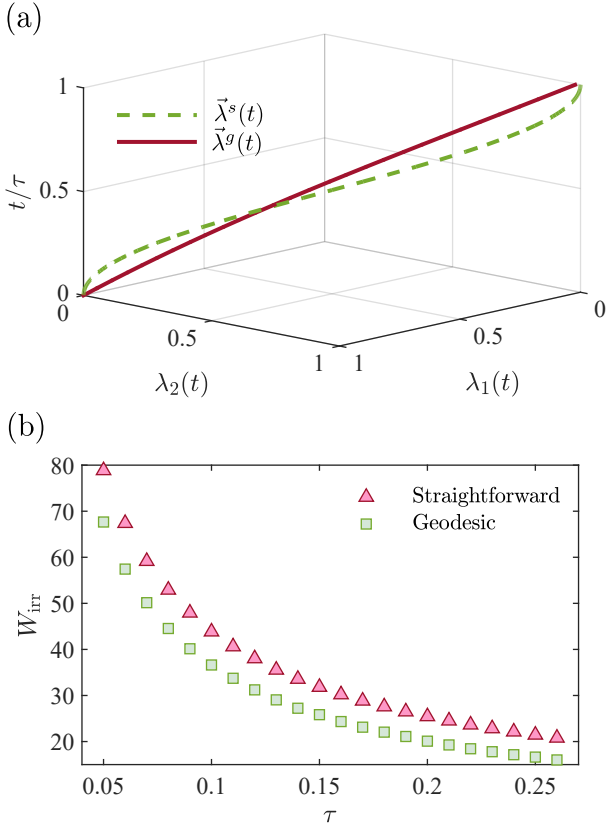


FIG. 3. (a) Geodesic protocols for the memory erasure process with the shortcut scheme. The control parameters vary from the initial value  $\vec{\lambda}(0) = (1, 0)$  to the final value  $\vec{\lambda}(\tau) = (0, 1)$ . The dashed lines represent the straightforward protocol while the solid lines represent the geodesic protocol. The geodesic protocol is obtained by solving the geodesic equation corresponding to the metric  $g_{\mu\nu}$ . (b) The irreversible energy cost of the straightforward protocol (red triangles) and the geodesic protocol (green squares). The energy cost of erasure processes given by the geodesic protocol is lower than that from the straightforward protocol.

approach for the shortcut scheme to be effective. With the application of tools from Riemannian geometry [52],

the procedure of searching the optimal erasure protocol is largely simplified with our two-step processes.

*Conclusions.* – In summary, we have developed a shortcut strategy to realize a finite-time one-bit memory erasure with minimal energy costs. In the shortcut scheme, an auxiliary control have been introduced to steer the system evolving along the path of instantaneous equilibrium states. We have employed the variational procedure to remove the momentum-dependent terms and derive an accessible auxiliary control. The irreversible energy cost of the erasure process have been minimized by adopting the geometric method that connects the optimal erasure protocol with the geodesic line in a Riemannian manifold. This property helps us to solve the optimal protocol by using methods developed in geometry. Numerical results have verified that the shortcut strategy can largely improve the accuracy of finite-time memory erasure without additional control means. Our strategy shall provide an effective design principle for finite-time memory erasure with low energy costs.

Recently, much effort has been devoted to realize the one-bit memory erasure with quasi-static control strategies [7–9, 20, 53]. The state lag accumulated in a finite-rate operation hinders the development of finite-time erasure schemes. Our strategy offers an operable approach to eliminate the nonequilibrium lag and realize the finite-time memory erasure with high accuracy and low energy costs. Besides, the Landauer’s bound have been approached in an underdamped micromechanical oscillator [20, 54]. The fast equilibrium recovery strategy have also been achieved with a levitated particle in the underdamped regime [55]. The driving force in our shortcut scheme only depends on the particle’s position. Therefore, it is promising to realize our finite-time memory erasure strategy with current experimental platforms.

*Acknowledgment.*—This work is supported by the National Natural Science Foundation of China (NSFC) (Grants No. 12088101, No. 11534002, No. 11875049, No. U1930402, No. U1930403 and No. 12047549) and the National Basic Research Program of China (Grant No. 2016YFA0301201).

- 
- [1] R. Landauer, IBM J. Res. Dev. **5**, 183 (1961).
  - [2] C. H. Bennett, IBM J. Res. Dev. **17**, 525 (1973).
  - [3] J. M. R. Parrondo, J. M. Horowitz, and T. Sagawa, Nat. Phys. **11**, 131 (2015).
  - [4] D. A. Pearlman and P. A. Kollman, J. Chem. Phys. **91**, 7831 (1989).
  - [5] R. H. Wood, J. Phys. Chem. **95**, 4838 (1991).
  - [6] R. Dillenschneider and E. Lutz, Phys. Rev. Lett. **102**, 210601 (2009).
  - [7] A. Bérut, A. Arakelyan, A. Petrosyan, S. Ciliberto, R. Dillenschneider, and E. Lutz, Nature **483**, 187 (2012).
  - [8] Y. Jun, M. Gavrilov, and J. Bechhoefer, Phys. Rev. Lett. **113**, 190601 (2014).
  - [9] A. Bérut, A. Petrosyan, and S. Ciliberto, J. Stat. Mech.: Theory Exp. **2015**, P06015 (2015).
  - [10] K. Proesmans, J. Ehrich, and J. Bechhoefer, Phys. Rev. Lett. **125**, 100602 (2020).
  - [11] K. Proesmans, J. Ehrich, and J. Bechhoefer, Phys. Rev. E **102**, 032105 (2020).
  - [12] A. B. Boyd, A. Patra, C. Jarzynski, and J. P. Crutchfield, J. Stat. Phys. **187** (2022), 10.1007/s10955-022-02871-0.
  - [13] R. Kawai, J. M. R. Parrondo, and C. V. den Broeck, Phys. Rev. Lett. **98**, 080602 (2007).
  - [14] A. Gomez-Marín, J. M. R. Parrondo, and C. V. den Broeck, Phys. Rev. E **78**, 011107 (2008).

- [15] S. Vaikuntanathan and C. Jarzynski, *Europhys. Lett.* **87**, 60005 (2009).
- [16] J. Horowitz and C. Jarzynski, *Phys. Rev. E* **79**, 021106 (2009).
- [17] G. Diana, G. B. Bagci, and M. Esposito, *Phys. Rev. E* **87**, 012111 (2013).
- [18] P. R. Zulkowski and M. R. DeWeese, *Phys. Rev. E* **89**, 052140 (2014).
- [19] P. R. Zulkowski and M. R. DeWeese, *Phys. Rev. E* **92**, 032113 (2015).
- [20] S. Dago, J. Pereda, N. Barros, S. Ciliberto, and L. Bellon, *Phys. Rev. Lett.* **126**, 170601 (2021).
- [21] T. V. Vu and K. Saito, *Phys. Rev. Lett.* **128**, 010602 (2022).
- [22] Y.-H. Ma, J.-F. Chen, C. P. Sun, and H. Dong, *Phys. Rev. E* **106**, 034112 (2022).
- [23] A. Rolandi and M. Perarnau-Llobet, *arXiv:2211.02065* (2022), 10.48550/arXiv.2211.02065.
- [24] A. Rolandi and M. Perarnau-Llobet, *arXiv:2306.16534* (2023), 10.48550/arXiv.2306.16534.
- [25] M. A. Miller and W. P. Reinhardt, *J. Chem. Phys.* **113**, 7035 (2000).
- [26] C. Jarzynski, *Phys. Rev. E* **65**, 046122 (2002).
- [27] S. Vaikuntanathan and C. Jarzynski, *Phys. Rev. Lett.* **100**, 190601 (2008).
- [28] D. D. L. Minh, *J. Chem. Phys.* **130**, 204102 (2009).
- [29] I. A. Martínez, A. Petrosyan, D. Guéry-Odelin, E. Trizac, and S. Ciliberto, *Nat. Phys.* **12**, 843 (2016).
- [30] A. Patra and C. Jarzynski, *New J. Phys.* **19**, 125009 (2017).
- [31] G. Li, H. T. Quan, and Z. C. Tu, *Phys. Rev. E* **96**, 012144 (2017).
- [32] J. A. C. Albay, S. R. Wulaningrum, C. Kwon, P.-Y. Lai, and Y. Jun, *Phys. Rev. Research* **1**, 033122 (2019).
- [33] J. A. C. Albay, P.-Y. Lai, and Y. Jun, *Appl. Phys. Lett.* **116**, 103706 (2020).
- [34] G. Li and Z. C. Tu, *Phys. Rev. E* **100**, 012127 (2019).
- [35] G. Li and Z. C. Tu, *Phys. Rev. E* **103**, 032146 (2021).
- [36] I. A. Martínez, É. Roldán, L. Dinis, and R. A. Rica, *Soft Matter* **13**, 22 (2017).
- [37] C. A. Plata, D. Guéry-Odelin, E. Trizac, and A. Prados, *J. Stat. Mech.: Theory Exp.* **2020**, 093207 (2020).
- [38] J.-F. Chen, *Phys. Rev. E* **106**, 054108 (2022).
- [39] X.-H. Zhao, Z.-N. Gong, and Z. C. Tu, *Phys. Rev. E* **106**, 064117 (2022).
- [40] G. Li, J.-F. Chen, C. P. Sun, and H. Dong, *Phys. Rev. Lett.* **128**, 230603 (2022).
- [41] G. Li, C. P. Sun, and H. Dong, *Phys. Rev. E* **107**, 014103 (2023).
- [42] S. S. Chittari and Z. Lu, *arXiv:2304.06822* (2023), 10.48550/arXiv.2304.06822.
- [43] K. Maruyama, F. Nori, and V. Vedral, *Reviews of Modern Physics* **81**, 1 (2009).
- [44] J. Bechhoefer, *Control Theory for Physicists* (Cambridge University Press, 2020) p. 500.
- [45] P. Salamon and R. S. Berry, *Phys. Rev. Lett.* **51**, 1127 (1983).
- [46] G. E. Crooks, *Phys. Rev. Lett.* **99**, 100602 (2007).
- [47] D. A. Sivak and G. E. Crooks, *Phys. Rev. Lett.* **108**, 190602 (2012).
- [48] J.-F. Chen, C. P. Sun, and H. Dong, *Phys. Rev. E* **104**, 034117 (2021).
- [49] D. Guéry-Odelin, A. Ruschhaupt, A. Kiely, E. Torrontegui, S. Martínez-Garaot, and J. Muga, *Rev. Mod. Phys.* **91**, 045001 (2019).
- [50] D. Guéry-Odelin, C. Jarzynski, C. A. Plata, A. Prados, and E. Trizac, *Rep. Prog. Phys.* **86**, 035902 (2023).
- [51] SupplementaryMaterials.
- [52] M. Berger, *A Panoramic View of Riemannian Geometry* (Springer Berlin Heidelberg, 2007).
- [53] M. Gavrilov and J. Bechhoefer, *Phys. Rev. Lett.* **117**, 200601 (2016).
- [54] S. Dago and L. Bellon, *Phys. Rev. Lett.* **128**, 070604 (2022).
- [55] D. Raynal, T. de Guillebon, D. Guéry-Odelin, E. Trizac, J.-S. Lauret, and L. Rondin, *arXiv:2303.09542* (2023), 10.48550/arXiv.2303.09542.

# Supplementary Material: A Shortcut to Finite-time Memory Erasure

Geng Li<sup>1,2</sup> and Hui Dong<sup>1,\*</sup>

<sup>1</sup>*Graduate School of China Academy of Engineering Physics, Beijing 100193, China*

<sup>2</sup>*School of Systems Science, Beijing Normal University, Beijing 100875, China*

The supplementary materials are devoted to provide detailed derivations in the main context.

## CONTENTS

I. The auxiliary control in shortcuts to memory erasure	1
A. Approximate shortcut scheme	1
B. An equivalent process with momentum-independent auxiliary control	2
II. Dimensionless form of the erasure process	3
III. Geodesic path for shortcuts to memory erasure	4
IV. The stochastic simulations	4
References	5

## I. THE AUXILIARY CONTROL IN SHORTCUTS TO MEMORY ERASURE

In this section, we will accomplish the finite-time memory erasure with the shortcut scheme. The momentum-dependent terms in the auxiliary control are removed by employing a variational method and a gauge transformation.

### A. Approximate shortcut scheme

We consider a one-bit memory system described by the Hamiltonian  $H_o(x, p, \vec{\lambda}) \equiv p^2/(2m) + U_o(x, \vec{\lambda})$  with the modulated double-well potential  $U_o(x, \vec{\lambda}) = kx^4 - A\lambda_1 x^2 - B\lambda_2 x$ . In the shortcut scheme, an auxiliary Hamiltonian  $H_a$  is added to steer the system evolving along the instantaneous equilibrium state  $P_{\text{eq}} = \exp[\beta(F - H_o)]$  during the finite-time erasure process with prescribed boundary conditions  $H_a(0) = H_a(\tau) = 0$ . The probability distribution  $P(x, p, t)$  of the microstate evolves according to the Kramers equation:

$$\frac{\partial P}{\partial t} = -\frac{\partial}{\partial x} \left( \frac{\partial H}{\partial p} P \right) + \frac{\partial}{\partial p} \left( \frac{\partial H}{\partial x} P + \gamma \frac{\partial H}{\partial p} P \right) + \frac{\gamma}{\beta} \frac{\partial^2 P}{\partial p^2}, \quad (1)$$

where  $H \equiv H_o + H_a$  represents the total Hamiltonian. The detailed derivation of the Kramers equation in the shortcut scheme is presented in Reference [1]. With the demand of instantaneous equilibrium paths, we derive the evolution equation for the auxiliary control:

$$\frac{\gamma}{\beta} \frac{\partial^2 H_a}{\partial p^2} - \frac{\gamma p}{m} \frac{\partial H_a}{\partial p} + \frac{\partial H_a}{\partial p} \frac{\partial H_o}{\partial x} - \frac{p}{m} \frac{\partial H_a}{\partial x} = \frac{dF}{dt} - \frac{\partial H_o}{\partial t}, \quad (2)$$

where the auxiliary Hamiltonian  $H_a(x, p, t)$  is proved to take the form  $H_a = \dot{\vec{\lambda}} \cdot \vec{f}$ . The boundary conditions of the auxiliary Hamiltonian  $H_a$  are satisfied with the request of  $\dot{\vec{\lambda}}(0) = \dot{\vec{\lambda}}(\tau) = 0$ .

With the modulated double-well potential  $U_o(x, \vec{\lambda})$ , it seems unlikely to solve Eq. (2) for the auxiliary Hamiltonian  $H_a$  analytically. We use a variational method [2, 3] to obtain an approximate auxiliary control  $H_a^* = \dot{\vec{\lambda}} \cdot \vec{f}^*(x, p, \vec{\lambda})$ , where  $\vec{f}^*$  denotes an approximation to  $\vec{f}$ . In the variational shortcut scheme, a functional is used to evaluate the approximation of the auxiliary control  $H_a^*$ . The variational functional is defined from Eq. (2) as

$$\mathcal{G}(H_a^*) = \int dx dp \left( \frac{\gamma}{\beta} \frac{\partial^2 H_a^*}{\partial p^2} - \frac{\gamma p}{m} \frac{\partial H_a^*}{\partial p} + \frac{\partial H_o}{\partial x} \frac{\partial H_a^*}{\partial p} - \frac{p}{m} \frac{\partial H_a^*}{\partial x} + \frac{\partial H_o}{\partial t} - \frac{dF}{dt} \right)^2 e^{-\beta H_o}. \quad (3)$$

The best possible form of the approximate auxiliary control is achieved from the variational equation  $\delta \mathcal{G}(H_a^*) / \delta H_a^* = 0$ .

Another difficulty of the underdamped shortcut scheme is the momentum-dependence in the auxiliary control. The momentum-dependent driving force is hard to be realized in the experimental setup due to the request to constantly monitor the particle's speed [4, 5]. With the help of the variational method and a gauge transformation, we remove the momentum-dependent terms in the auxiliary control. We firstly remove the high-order momentum-dependent terms by using the variational method. We assume that the variational auxiliary Hamiltonian takes the form as

$$H_a^* = \dot{\lambda}_1(a_4 x p + a_3 p + a_2 x^2 + a_1 x) + \dot{\lambda}_2(b_4 x p + b_3 p + b_2 x^2 + b_1 x), \quad (4)$$

where  $a_n \equiv a_n(\vec{\lambda})$  and  $b_n \equiv b_n(\vec{\lambda})$  with  $n = 1, 2, 3, 4$  are functions to be determined in the variational procedure. With the specified form of the auxiliary control in Eq. (4), the variational operation over  $H_a^*$  is converted to the partial-derivative operation over parameters  $a_n \equiv a_n(\vec{\lambda})$  and  $b_n \equiv b_n(\vec{\lambda})$  with  $n = 1, 2, 3, 4$ .

### B. An equivalent process with momentum-independent auxiliary control

Note that there are still linear momentum-dependent terms in the variational auxiliary Hamiltonian (4). In the variational shortcut scheme employing the Hamiltonian  $H = H_o + H_a^*$ , the particle's evolution is governed by the Langevin equation

$$\begin{aligned} \dot{x} &= \frac{p}{m} + \dot{\lambda}_1(a_4 x + a_3) + \dot{\lambda}_2(b_4 x + b_3), \\ \dot{p} &= -4kx^3 + 2A\lambda_1 x + B\lambda_2 - \dot{\lambda}_1(a_4 p + 2a_2 x + a_1) - \dot{\lambda}_2(b_4 p + 2b_2 x + b_1) - \gamma \dot{x} + \xi(t), \end{aligned} \quad (5)$$

where  $\xi(t)$  represents the Gaussian white noise. The measurement difficulties of the momentum-dependent forces in Eq. (5) impede practical implementations of the shortcut scheme experimentally [4, 5].

We introduce a gauge transformation  $X = x$  and  $P = p + m\dot{\lambda}_1(a_4 x + a_3) + m\dot{\lambda}_2(b_4 x + b_3)$  to obtain an equivalent process with the variables  $X$  and  $P$  under the evolution as follows

$$\begin{aligned} \dot{X} &= \frac{P}{m}, \\ \dot{P} &= -\frac{\partial U_o}{\partial X} - \frac{\partial U_a}{\partial X} - \gamma \dot{X} + \xi(t). \end{aligned} \quad (6)$$

Here the auxiliary potential for these new variables is  $U_a(X, t) = C_2(t)X^2 + C_1(t)X$  with the parameters

$$\begin{aligned} C_2(t) &= \dot{\lambda}_1 a_2 + \dot{\lambda}_2 b_2 - \frac{m}{2}(\ddot{\lambda}_1 a_4 + \ddot{\lambda}_2 b_4 + \dot{\lambda}_1^2 \frac{\partial a_4}{\partial \lambda_1} + \dot{\lambda}_1^2 a_4^2 + \dot{\lambda}_2^2 \frac{\partial b_4}{\partial \lambda_2} + \dot{\lambda}_2^2 b_4^2 + \dot{\lambda}_1 \dot{\lambda}_2 \frac{\partial a_4}{\partial \lambda_2} + \dot{\lambda}_1 \dot{\lambda}_2 \frac{\partial b_4}{\partial \lambda_1} + 2\dot{\lambda}_1 \dot{\lambda}_2 a_4 b_4), \\ C_1(t) &= \dot{\lambda}_1 a_1 + \dot{\lambda}_2 b_1 - m(\ddot{\lambda}_1 a_3 + \ddot{\lambda}_2 b_3 + \dot{\lambda}_1^2 \frac{\partial a_3}{\partial \lambda_1} + \dot{\lambda}_1^2 a_3 a_4 + \dot{\lambda}_2^2 \frac{\partial b_3}{\partial \lambda_2} + \dot{\lambda}_2^2 b_3 b_4 + \dot{\lambda}_1 \dot{\lambda}_2 \frac{\partial a_3}{\partial \lambda_2} + \dot{\lambda}_1 \dot{\lambda}_2 \frac{\partial b_3}{\partial \lambda_1} \\ &\quad + \dot{\lambda}_1 \dot{\lambda}_2 b_3 a_4 + \dot{\lambda}_1 \dot{\lambda}_2 a_3 b_4). \end{aligned} \quad (7)$$

With the operation of Jacobi's transformation, we find that the system's distribution in this equivalent process follows a fixed pattern as

$$P_f(X, P, t) = \exp \left\{ \beta \left[ F - \frac{1}{2m} (P - m\partial H_a^* / \partial P)^2 - U_o \right] \right\}. \quad (8)$$

Compared with the instantaneous equilibrium distribution  $P_{eq} = \exp[\beta(F - H_o)]$ , the extra term  $m\partial H_a^* / \partial P$  in the fixed distribution  $P_f$  vanishes with the consideration of the boundary conditions  $\dot{\vec{\lambda}}(0) = \dot{\vec{\lambda}}(\tau) = 0$ . Therefore, the system's distribution  $P_f$  returns to the instantaneous equilibrium distribution  $P_{eq}$  at the beginning  $t = 0$  and end  $t = \tau$  of the equivalent process with the Hamiltonian  $H = H_o + U_a$ .

## II. DIMENSIONLESS FORM OF THE ERASURE PROCESS

In this section, we numerically solve the function  $f^*$  for the auxiliary control. For later simulations, we introduce the characteristic length  $l_c \equiv (k_B T/k)$ , the characteristic times  $\tau_1 = m/\gamma$  and  $\tau_2 = \gamma/(kl_c^2)$  to define the dimensionless coordinate  $\tilde{x} \equiv x/l_c$ , momentum  $\tilde{p} \equiv p\tau_2/(ml_c)$ , time  $s \equiv t/\tau_2$ , and the parameters  $\tilde{A} \equiv A/(kl_c^2)$  and  $\tilde{B} \equiv B/(kl_c^3)$ . The dimensionless evolution equation for the auxiliary control follows as

$$\frac{1}{\alpha^2} \frac{\partial^2 \tilde{H}_a}{\partial \tilde{p}^2} - \frac{1}{\alpha} \tilde{p} \frac{\partial \tilde{H}_a}{\partial \tilde{p}} + \frac{1}{\alpha} \frac{\partial \tilde{H}_a}{\partial \tilde{p}} \frac{\partial \tilde{H}_o}{\partial \tilde{x}} - \tilde{p} \frac{\partial \tilde{H}_a}{\partial \tilde{x}} = \frac{d\tilde{F}}{ds} - \frac{\partial \tilde{H}_o}{\partial s}, \quad (9)$$

with the dimensionless parameter  $\alpha \equiv \tau_1/\tau_2$  and the dimensionless Hamiltonian  $\tilde{H}_o \equiv H_o/(k_B T)$  and  $\tilde{H}_a \equiv H_a/(k_B T)$ . The dimensionless variational functional takes the form

$$\tilde{\mathcal{G}}(\tilde{H}_a^*) = \int d\tilde{x} d\tilde{p} \left( \frac{1}{\alpha^2} \frac{\partial^2 \tilde{H}_a}{\partial \tilde{p}^2} - \frac{1}{\alpha} \tilde{p} \frac{\partial \tilde{H}_a}{\partial \tilde{p}} + \frac{1}{\alpha} \frac{\partial \tilde{H}_a}{\partial \tilde{p}} \frac{\partial \tilde{H}_o}{\partial \tilde{x}} - \tilde{p} \frac{\partial \tilde{H}_a}{\partial \tilde{x}} + \frac{\partial \tilde{H}_o}{\partial s} - \frac{\partial \tilde{H}_a}{\partial s} \right)^2 e^{-\tilde{H}_o}, \quad (10)$$

with the dimensionless variational auxiliary Hamiltonian

$$\tilde{H}_a^* = \lambda_1' (\tilde{a}_4 \tilde{x} \tilde{p} + \tilde{a}_3 \tilde{p} + \tilde{a}_2 \tilde{x}^2 + \tilde{a}_1 \tilde{x}) + \lambda_2' (\tilde{b}_4 \tilde{x} \tilde{p} + \tilde{b}_3 \tilde{p} + \tilde{b}_2 \tilde{x}^2 + \tilde{b}_1 \tilde{x}). \quad (11)$$

Here  $\lambda_1' \equiv d\lambda_1/ds$ ,  $\lambda_2' \equiv d\lambda_2/ds$  and the parameters  $\tilde{a}_n$  and  $\tilde{b}_n$  are the dimensionless version of  $a_n$  and  $b_n$  with  $n = 1, 2, 3, 4$ .

With the variational procedure of  $\tilde{\mathcal{G}}(\tilde{H}_a^*)$  over the parameters  $\tilde{a}_n$  and  $\tilde{b}_n$ , we obtain the set of equations as

$$\begin{aligned} [48\langle \tilde{x}^4 \rangle + (\frac{1}{\alpha} - 16\lambda_1)\langle \tilde{x}^2 \rangle + 3]\tilde{a}_4 + [48\langle \tilde{x}^3 \rangle + (\frac{1}{\alpha} - 16\lambda_1)\langle \tilde{x} \rangle]\tilde{a}_3 + 2\langle \tilde{x}^2 \rangle \tilde{a}_2 + \langle \tilde{x} \rangle \tilde{a}_1 &= 16\alpha \langle \tilde{x}^2 \rangle, \\ [48\langle \tilde{x}^3 \rangle + (\frac{1}{\alpha} - 16\lambda_1)\langle \tilde{x} \rangle]\tilde{a}_4 + [48\langle \tilde{x}^2 \rangle + (\frac{1}{\alpha} - 16\lambda_1)]\tilde{a}_3 + 2\langle \tilde{x} \rangle \tilde{a}_2 + \tilde{a}_1 &= 16\alpha \langle \tilde{x} \rangle, \\ \frac{\langle \tilde{x}^2 \rangle}{\alpha} \tilde{a}_4 + \frac{\langle \tilde{x} \rangle}{\alpha} \tilde{a}_3 + 2\langle \tilde{x}^2 \rangle \tilde{a}_2 + \langle \tilde{x} \rangle \tilde{a}_1 &= 0, \\ \frac{\langle \tilde{x} \rangle}{\alpha} \tilde{a}_4 + \frac{1}{\alpha} \tilde{a}_3 + 2\langle \tilde{x} \rangle \tilde{a}_2 + \tilde{a}_1 &= 0, \\ [48\langle \tilde{x}^4 \rangle + (\frac{1}{\alpha} - 16\lambda_1)\langle \tilde{x}^2 \rangle + 3]\tilde{b}_4 + [48\langle \tilde{x}^3 \rangle + (\frac{1}{\alpha} - 16\lambda_1)\langle \tilde{x} \rangle]\tilde{b}_3 + 2\langle \tilde{x}^2 \rangle \tilde{b}_2 + \langle \tilde{x} \rangle \tilde{b}_1 &= 16\alpha \langle \tilde{x} \rangle, \\ [48\langle \tilde{x}^3 \rangle + (\frac{1}{\alpha} - 16\lambda_1)\langle \tilde{x} \rangle]\tilde{b}_4 + [48\langle \tilde{x}^2 \rangle + (\frac{1}{\alpha} - 16\lambda_1)]\tilde{b}_3 + 2\langle \tilde{x} \rangle \tilde{b}_2 + \tilde{b}_1 &= 16\alpha, \\ \frac{\langle \tilde{x}^2 \rangle}{\alpha} \tilde{b}_4 + \frac{\langle \tilde{x} \rangle}{\alpha} \tilde{b}_3 + 2\langle \tilde{x}^2 \rangle \tilde{b}_2 + \langle \tilde{x} \rangle \tilde{b}_1 &= 0, \\ \frac{\langle \tilde{x} \rangle}{\alpha} \tilde{b}_4 + \frac{1}{\alpha} \tilde{b}_3 + 2\langle \tilde{x} \rangle \tilde{b}_2 + \tilde{b}_1 &= 0, \end{aligned} \quad (12)$$

where  $\langle \tilde{x}^n \rangle \equiv \int_{-\infty}^{+\infty} \tilde{x}^n \exp(-\tilde{U}_o) d\tilde{x} / \int_{-\infty}^{+\infty} \exp(-\tilde{U}_o) d\tilde{x}$  with  $n = 1, 2, 3, 4$ . We first numerically obtain the values of  $\langle \tilde{x}^n \rangle$  for different values of control parameters  $\lambda_1$  and  $\lambda_2$ . According to the boundary conditions of  $\lambda_1$  and  $\lambda_2$ , we set the range of control parameters to be  $\lambda_1 \in [-5, 5]$  and  $\lambda_2 \in [-5, 5]$ . Second, we numerically solve the set of Eqs. (12) for different values of  $\langle \tilde{x}^n \rangle$  marked by different set of control parameters  $\lambda_1$  and  $\lambda_2$ . In this way, we obtain the corresponding solutions of  $\tilde{a}_n$  and  $\tilde{b}_n$  for different set of control parameters  $\lambda_1$  and  $\lambda_2$ . Finally, we fit the polynomial relation between the coefficients  $\tilde{a}_n$ ,  $\tilde{b}_n$  and the parameters  $\lambda_1$ ,  $\lambda_2$ .

The dimensionless auxiliary potential takes the form as

$$\tilde{U}_a(\tilde{X}, s) = \tilde{C}_2(s) \tilde{X}^2 + \tilde{C}_1(s) \tilde{X}, \quad (13)$$



where the dimensionless parameters follow as

$$\begin{aligned}\tilde{C}_2(s) &= \lambda'_1 \tilde{a}_2 + \lambda'_2 \tilde{b}_2 - \frac{1}{2}(\lambda''_1 \tilde{a}_4 + \lambda''_2 \tilde{b}_4 + \lambda'^2_1 \frac{\partial \tilde{a}_4}{\partial \lambda_1} + \frac{1}{\alpha} \lambda'^2_1 \tilde{a}_4^2 + \lambda'^2_2 \frac{\partial \tilde{b}_4}{\partial \lambda_2} + \frac{1}{\alpha} \lambda'^2_2 \tilde{b}_4^2 + \lambda'_1 \lambda'_2 \frac{\partial \tilde{a}_4}{\partial \lambda_2} + \lambda'_1 \lambda'_2 \frac{\partial \tilde{b}_4}{\partial \lambda_1} + \frac{2}{\alpha} \lambda'_1 \lambda'_2 \tilde{a}_4 \tilde{b}_4), \\ \tilde{C}_1(s) &= \lambda'_1 \tilde{a}_1 + \lambda'_2 \tilde{b}_1 - \lambda''_1 \tilde{a}_3 - \lambda''_2 \tilde{b}_3 - \lambda'^2_1 \frac{\partial \tilde{a}_3}{\partial \lambda_1} - \frac{1}{\alpha} \lambda'^2_1 \tilde{a}_3 \tilde{a}_4 - \lambda'^2_2 \frac{\partial \tilde{b}_3}{\partial \lambda_2} - \frac{1}{\alpha} \lambda'^2_2 \tilde{b}_3 \tilde{b}_4 - \lambda'_1 \lambda'_2 \frac{\partial \tilde{a}_3}{\partial \lambda_2} - \lambda'_1 \lambda'_2 \frac{\partial \tilde{b}_3}{\partial \lambda_1} \\ &\quad - \frac{1}{\alpha} \lambda'_1 \lambda'_2 \tilde{b}_3 \tilde{a}_4 - \frac{1}{\alpha} \lambda'_1 \lambda'_2 \tilde{a}_3 \tilde{b}_4.\end{aligned}\tag{14}$$

### III. GEODESIC PATH FOR SHORTCUTS TO MEMORY ERASURE

In this section, we use geometric approach to find the geodesic path with minimal energy costs for the erasure process controlled by the shortcut scheme. With the variational auxiliary Hamiltonian in Eq. (11), we obtain the dimensionless metric for the parametric space as

$$\tilde{g} = \begin{pmatrix} \tilde{a}_4^2 \langle \tilde{x}^2 \rangle + 2\tilde{a}_3 \tilde{a}_4 \langle \tilde{x} \rangle + \tilde{a}_3^2 & \tilde{a}_4 \tilde{b}_4 \langle \tilde{x}^2 \rangle + (\tilde{a}_3 \tilde{b}_4 + \tilde{b}_3 \tilde{a}_4) \langle \tilde{x} \rangle + \tilde{a}_3 \tilde{b}_3 \\ \tilde{a}_4 \tilde{b}_4 \langle \tilde{x}^2 \rangle + (\tilde{a}_3 \tilde{b}_4 + \tilde{b}_3 \tilde{a}_4) \langle \tilde{x} \rangle + \tilde{a}_3 \tilde{b}_3 & \tilde{b}_4^2 \langle \tilde{x}^2 \rangle + 2\tilde{b}_3 \tilde{b}_4 \langle \tilde{x} \rangle + \tilde{b}_3^2 \end{pmatrix}.\tag{15}$$

The polynomial relation between the metric  $\tilde{g}_{\mu\nu}$  and the parameters  $\lambda_1, \lambda_2$  is fitted by substituting the values of  $\tilde{a}_n, \tilde{b}_n$ , and  $\langle \tilde{x}^n \rangle$  into Eq. (15).

According to the geometric approach presented in the main text, the task of finding optimal erasure protocol with minimal energy costs is equivalent to solving the geodesic path in the parametric space with the metric  $\tilde{g}_{\mu\nu}$ . The geodesic path is obtained by solving the geodesic equation

$$\ddot{\lambda}_\mu + \sum_{\nu\kappa} \Gamma_{\nu\kappa}^\mu \dot{\lambda}_\nu \dot{\lambda}_\kappa = 0,\tag{16}$$

with the given boundary conditions  $\vec{\lambda}(0) = (1, 0)$  and  $\vec{\lambda}(\tau) = (0, 1)$ . Here the Christoffel symbol is defined as  $\Gamma_{\nu\kappa}^\mu \equiv \frac{1}{2} \sum_\iota (\tilde{g}^{-1})_{\iota\mu} (\partial_{\lambda_\kappa} \tilde{g}_{\iota\nu} + \partial_{\lambda_\nu} \tilde{g}_{\iota\kappa} - \partial_{\lambda_\iota} \tilde{g}_{\nu\kappa})$ . We employ the shooting method [6] to numerically solve the geodesic equation. The two-point boundary values problem is treated as an initial value problem

$$\ddot{\lambda}_\mu = y_\mu(t, \vec{\lambda}, \dot{\vec{\lambda}}) \equiv \frac{1}{2} \sum_{\nu\kappa\iota} (g^{-1})_{\iota\mu} \left( \frac{\partial g_{\nu\kappa}}{\partial \lambda_\iota} - \frac{\partial g_{\iota\nu}}{\partial \lambda_\kappa} - \frac{\partial g_{\iota\kappa}}{\partial \lambda_\nu} \right) \dot{\lambda}_\nu \dot{\lambda}_\kappa,\tag{17}$$

with the initial conditions  $\vec{\lambda}(0) = (1, 0)$  and  $\dot{\vec{\lambda}}(0) = \vec{d}$ . Here  $\vec{d}$  is the initial rate that is constantly updated until the solution of Eq. (17) reaches the required position  $\vec{\lambda}(\tau) = (0, 1)$ . In the simulation, we use the Euler algorithm to solve the geodesic equation (17). The Newton's method is taken to iterate the initial rate  $\vec{d}$  and finally satisfy the boundary condition  $\vec{\lambda}(\tau) = (0, 1)$ .

### IV. THE STOCHASTIC SIMULATIONS

In this section, we introduce the algorithm to simulate the erasure process and obtain the mean work. The motion of the memory system is described by the Langevin equation in Eq. (6). The dimensionless version of this equation follows as

$$\begin{aligned}\tilde{X}' &= \tilde{P}, \\ \tilde{P}' &= -\frac{1}{\alpha} \frac{\partial \tilde{U}_o}{\partial \tilde{X}} - \frac{1}{\alpha} \frac{\partial \tilde{U}_a}{\partial \tilde{X}} - \frac{\tilde{P}}{\alpha} + \frac{\sqrt{2}}{\alpha} \zeta(s),\end{aligned}\tag{18}$$

where  $\zeta(s)$  is a Gaussian white noise satisfying  $\langle \zeta(s) \rangle = 0$  and  $\langle \zeta(s_1) \zeta(s_2) \rangle = \delta(s_1 - s_2)$ . The Langevin equation (18) is solved by employing the Euler algorithm as

$$\begin{aligned}\tilde{X}(s + \delta s) &= \tilde{X}(s) + \tilde{P} \delta s, \\ \tilde{P}(s + \delta s) &= \tilde{P}(s) - \frac{1}{\alpha} \frac{\partial \tilde{U}_o}{\partial \tilde{X}} \delta s - \frac{1}{\alpha} \frac{\partial \tilde{U}_a}{\partial \tilde{X}} \delta s - \frac{\tilde{P}}{\alpha} \delta s + \frac{\sqrt{2\delta s}}{\alpha} \theta(s),\end{aligned}\tag{19}$$

where  $\delta s$  is the time step and  $\theta(s)$  is a random number sampled from Gaussian distribution with zero mean and unit variance. The work of the system's stochastic trajectory follows as

$$\begin{aligned}\tilde{w} \equiv \frac{w}{k_B T} &= \int_0^1 \left( \frac{\partial \tilde{H}_o}{\partial s} + \frac{\partial \tilde{U}_a}{\partial s} \right) ds \\ &\approx \sum \left( \frac{\partial \tilde{H}_o}{\partial s} + \frac{\partial \tilde{U}_a}{\partial s} \right) \delta s.\end{aligned}\tag{20}$$

In the simulation, we have chosen the parameters  $\vec{\lambda}(0) = (1, 0)$ ,  $\vec{\lambda}(\tau) = (0, 1)$ ,  $k_B T = 1$ ,  $\gamma = 1$ , and  $m = 0.01$ . The mean work is obtained as the ensemble average over the trajectory work of  $10^5$  stochastic trajectories.

---

\* hdong@gscaep.ac.cn

- [1] Geng Li, Jin-Fu Chen, C. P. Sun, and Hui Dong. Geodesic path for the minimal energy cost in shortcuts to isothermality. *Phys. Rev. Lett.*, 128(23):230603, jun 2022.
- [2] Geng Li and Z. C. Tu. Equilibrium free-energy differences from a linear nonequilibrium equality. *Phys. Rev. E*, 103(3):032146, mar 2021.
- [3] Geng Li, C. P. Sun, and Hui Dong. Geodesic path for the optimal nonequilibrium transition: Momentum-independent protocol. *Phys. Rev. E*, 107(1):014103, jan 2023.
- [4] D. Guéry-Odelin, A. Ruschhaupt, A. Kiely, E. Torrontegui, S. Martínez-Garaot, and J. G. Muga. Shortcuts to adiabaticity: Concepts, methods, and applications. *Rev. Mod. Phys.*, 91(4):045001, oct 2019.
- [5] David Guéry-Odelin, Christopher Jarzynski, Carlos A Plata, Antonio Prados, and Emmanuel Trizac. Driving rapidly while remaining in control: classical shortcuts from hamiltonian to stochastic dynamics. *Rep. Prog. Phys.*, 86(3):035902, jan 2023.
- [6] Marcel Berger. *A Panoramic View of Riemannian Geometry*. Springer Berlin Heidelberg, June 2007.